Preprint Declaration

Title: High-resolution pavement material data can improve estimates of water supply from precipitation to street trees

Authors:

Moreen Willaredt[a,b] (mwillaredt@ucdavis.edu)

Dagmar Haase[b,c] (dagmar.haase@hu-berlin.de)

Alessandro Ossola[a] (aossola@ucdavis.edu)

[a] Department of Plant Sciences, University of California Davis, One Shields Avenue, Davis, 95616, CA, USA

[b] Department of Geography, Humboldt-Universität zu Berlin, Berlin, 10117, Germany

[c] Helmholtz Centre for Environmental Research UFZ, Department of Computational Landscape Ecology, Leipzig, 04318, Germany

This paper is currently under review and at this stage a non-peer reviewed preprint submitted to EarthArXiv. The manuscript is under review in the Journal Landscape and Urban Planning and contains improvements acknowledging the comments provided during the first review round of two anonymous reviewers.

Highlights

High-resolution pavement material data can improve estimates of water supply from precipitation to street trees

Moreen Willaredt, Dagmar Haase, Alessandro Ossola

- Widely used satellite-derived data underestimates imperviousness in tree catchments.
- Pavement material layouts cause variability that undermines imperviousness as an accurate predictor for infiltration reduction.
- High-resolution data, that detail pavement material, facilitate identification of street trees for which infiltration reduction compromises water supply to meet transpiration demand.
- Both de-paving and the exchange of pavement material could increase water supply substantially.

High-resolution pavement material data can improve estimates of water supply from precipitation to street trees

Moreen Willaredt[a,b,*], Dagmar Haase[b,c], Alessandro Ossola[a]

[a] *Department of Plant Sciences, University of California Davis, PES-1238, One Shields Avenue, Davis, 95616, CA, USA*
[b] *Department of Geography, Humboldt-Universität zu Berlin, Berlin, 10117, Germany*
[c] *Helmholtz Centre for Environmental Research UFZ, Department of Computational Landscape Ecology, Leipzig, 04318, Germany*

Abstract

Impervious surfaces in urban landscapes strongly influence how precipitation supplies water to trees. Most data on imperviousness are satellite-derived restricting our ability to analyze impacts of imperviousness at the scale of single tree catchments: the area covering tree roots. To address this challenge, we compiled a high-resolution dataset for Berlin, Germany, that specifies pavement materials, complementing it with hydrologic properties from the literature. Our approach aims to assess the accuracy of satellite-derived imperviousness in 71,311 tree catchments and analyze infiltration reduction due to the presence of pavement at the local, fine scale.

We found substantial disagreement with satellite-derived imperviousness for $\approx 99\,\%$ of tree catchments and that satellite-derived data on average underestimates imperviousness by $13.1\,\%$. High-resolution imperviousness correlated with reduced infiltration, yet catchments with similar impervious-

*Corresponding author: Moreen Willaredt, moreenwillaredt@posteo.de

ness exhibited high variability and even bimodal distributions. These patterns can be explained by the dominant pavement material, highlighting the importance of high-resolution imperviousness data that capture pavement materials when assessing urban stormwater dynamics. In Berlin the mean annual infiltration reduction was 45.9 %, sometimes limiting water availability for *Tilia* below transpiration demand during the growing season. These results indicate that street trees in paved environments might experience modified climatic and hydraulic regimes decoupled from those dictated by regional climates. Our findings can help refine predictions of tree drought stress and stimulate field studies along imperviousness gradients. The outcomes can inform practice, e.g. tree water management, and climate adaptation strategies in urban planning, such as pavement removal or retrofitting of tree planting sites.

Keywords: Street trees, Imperviousness, Pavement, Stormwater infiltration, Water management, Open data

1. Introduction

Pavement and soil sealing are key features of urban landscapes and disrupt the functions of the soil involved in regulating water cycles and energy balance in urban environments (Timm et al., 2018; Scalenghe and Marsan, 2009). Pavements above the root zone of urban trees directly affect the water supply from precipitation (Whitlow and Bassuk, 1987; Wessolek and

Kluge, 2021; Tams et al., 2024) and the temperature surrounding trees (Kjelgren, 1993; Moser-Reischl et al., 2019) and therefore their evapotranspiration rate, water demand, and ultimately hydraulic stress and failures. Sustaining healthy mature trees that provide evaporative cooling and shade has become an urgent challenge under increased heat and recurrent meteorological drought (Velasquez-Camacho et al., 2025; Rosenberger et al., 2024; Haa, a; Marchin et al., 2021). In a changing climate and in urban environments where extreme events are often exacerbated by urban heat islands (UHIs) and soil sealing (de la Mota Daniel et al., 2018; Moser et al., 2016; Mullaney et al., 2015; Savi et al., 2014), additional water supply can be required to guarantee the survival of trees and entire urban forests (Rosenberger et al., 2025; Tams et al., 2024).

The relationship between the built environment and tree growth, beyond natural climatic drivers, such as precipitation and temperature, remains an open question to date (Esperon-Rodriguez et al., 2025). Some studies note smaller changes in leaf water potential and sap flow during drier periods, in trees growing in impervious sites (Rissanen et al., 2025; Cinto Mejía et al., 2025). High-resolution assessments of soil sealing in tree catchments can facilitate identifying pavement layouts that support tree survival and long-term growth. This is crucial for reaching urban forestry benchmarks, such as the 3-30-300 rule (Browning et al., 2024; Croeser et al., 2024), which advocates for every city resident to see at least 3 trees from their home, for 30% canopy cover in every neighborhood, and for 300 meters access to a green

space. Achieving these targets requires not only the planting of new trees, but also the establishment of growing conditions and management strategies that sustain urban trees over the long term. Only trees that reach maturity can deliver their intended ecosystem services and meet the goals of urban greening programs.

Further, this knowledge is needed to address the question whether removing and or exchanging pavement in tree catchments could partially compensate for increasing drought periods in our cities.

Soil sealing is defined as "the covering of soils with an artificial impervious surface" (Tobias et al., 2018). It is quantified by the degree of soil sealing or imperviousness density —the percentage of the built-up area. The resolution of openly available datasets of urban imperviousness in the world's cities and towns ranges between 1-30 m, albeit most dataset have a spatial resolution of over 10-15 m. High resolution data are available, e.g. for some cities in coastal region of the US (National Oceanic and Atmospheric Administration, Office for Coastal Management, 2025). Global datasets, e.g. the Global Human Settlement Layer (GHSL) or global impervious surface area (GISA) exist at 10 or 30 m resolution (Huang et al., 2022). Where tree canopies largely obscure surfaces underneath, deep learning models together with post-processing algorithms were able to recover 4 km^2 (1 %) of undetected impervious surfaces obscured by tree canopies in a case study in Corpus Christie, TX (Techapinyawat et al., 2024). These developments can substantially contribute to improved identification of impervious surfaces,

given the availability of high-resolution aerial imagery, which can be costly.

Despite the increase in spatial resolution of remotely sensed imperviousness data, the level of detail is often too low to identify different pavement materials. Consequently, all built elements in the urban fabric are assumed to be fully impervious. However, not all artificial surfaces mapped as impervious completely prevent the infiltration of precipitation; their permeability greatly varies depending on the material used (Timm et al., 2018; Schaffitel et al., 2020). Consequently, materials might impact the water supply in tree catchments in disparate ways. Timm et al. (2018) distinguished four pavement classes that reflect the pavement material specific degree of sealing. Their review emphasizes the capacity of several pavement materials (e.g., small stone pavers, large concrete pavers) to infiltrate more than 50 % of the annual precipitation in moist mid-latitude climates. Even asphalt is reported to infiltrate low amounts of precipitation, especially in the case when it is damaged. This observed permeability is crucial when analyzing the localized effects of pavements on urban tree water supply. Hence, greater level of detail is needed to more robustly measure the impact of pavements on the water supply in urban tree catchments. Kluge and Kirmaier (2024) manually mapped existing pavement layouts (the combination of pavement materials and their shares in each catchment) in tree catchments of 49 trees investing a substantial amount of fieldwork. Hence, the intensity of labor often inhibits the manual mapping of large urban areas, required to account for a high variability of pavement layouts across the city.

A new source for urban high-resolution imperviousness data are open data platforms provided by some municipalities. Some of the data describing the public space (e.g. road networks, public green spaces), include detailed information on the extent of different road segments, and in some cases, the pavement materials or pavement condition. The City of Berlin, Germany, conducted an extensive survey in 2014-2015 mapping and digitizing the entire public space of Berlin (Senatsverwaltung für Stadtentwicklung und Wohnen Berlin, 2014). The City of Melbourne, Australia, provides a similar dataset reflecting the condition of its road segments (City of Melbourne, 2016). An increasing number of cities invest in smart city strategies including the assimilation and provision of open data and digital twins (Gracias et al., 2023). This trend promises to provide valuable sources of accurate data on imperviousness at very small, metric, scales. In this study Berlin's rare digital representation is curated and harnessed for mapping imperviousness in the immediate surrounding of trees planted across the city. The study specifically aims to addresses the following research questions: i) Do satellite-derived imperviousness data accurately reflect imperviousness on the metric scale of single street trees? ii) To what extent can imperviousness be used to estimate reductions in stormwater infiltration in urban tree catchments? and iii) How does reduced infiltration affect water supply across planted tree genera in Berlin, and, using the most abundant genera as a case study, can infiltration reduction in a given year lead to a shortage relative to transpiration demand during the vegetation season?

2. Methods

2.1. Study Location

The study was conducted around street trees growing across the city of Berlin, Germany (52°27′N, 13°19′E). Berlin is the largest city in Germany with a growing population of almost 3.8 million people (Amt für Statistik Berlin-Brandenburg, 2025). It is heterogeneous across its planning units (neighborhood scale) in urban form, population, street tree density, and diversity (see Table 1). The pavement materials on roads and sidewalks in Berlin's public space are diverse (Table 2) and reflect the complex (re)development history in the last few centuries .

Table 1: Ranges of variables heterogeneity across Berlin's urban planning units at the neighborhood scale (Senatsverwaltung für Stadtentwicklung und Wohnen, 2021)

Property	min	mean	max	sd
Population density (people ha^{-1})	60	4,753	14,380	2,659
Street trees (n)	3	711	5,289	584
Imperviousness (%)	7	47	85	16
Tree genus diversity (n)	1	17	47	7

The datasets used in this study are listed in the Appendix in Table A.4 with respective references and specifications about type and projections.

2.2. Tree catchment scale

The characteristics of the immediate surrounding of trees, including the degree of sealing, have been included as a variable in previous modeling and field studies, focusing on urban tree growth, the provision of cooling or the

demand for tree water (Rosenberger et al., 2024; Tams et al., 2023; Wessolek and Kluge, 2021; Kluge and Kirmaier, 2024; Rosenberger et al., 2024; Moser et al., 2016). The spatial extension of local single tree scales in these studies span a range between the tree pit size ($8\,\mathrm{m}^2$) (Rosenberger et al., 2024), the urban entity of an entire public square (Moser et al., 2016), up to a landscape scale of 500 m radius (Pattnaik et al., 2024). Many studies use the projected canopy size or drip line to delineate the immediate tree environment (Vrecenak et al., 1989; Wessolek and Kluge, 2021; Tams et al., 2024; Gillner et al., 2014), or 1.5 time the canopy projection (Sand et al., 2018). This study focuses on the reduction of potential stormwater infiltration caused by the presence of man-made structures, e.g. pavement. We therefore define the tree catchment scale to be the area, and respective soil volume, where water infiltrates to the tree root zone. In urban environments, the rood spread is resulting from the complex interplay between tree species traits and physical constraints defined by built structures, e.g. curbs, roads or buildings and compacted soil (Grabosky and Bassuk, 1995; Watson et al., 2014). Day et al. (2010) report, that the roots in urban environments might extend beyond the canopy dripline. They summarized studies that included 38 species and derived an empirical relationship between the maximum spread of the root (r in m) and the diameter in breast height (DBH in cm):

$$r = 5.266 \cdot \left(1 - e^{-0.096\,\mathrm{DBH}}\right) \tag{1}$$

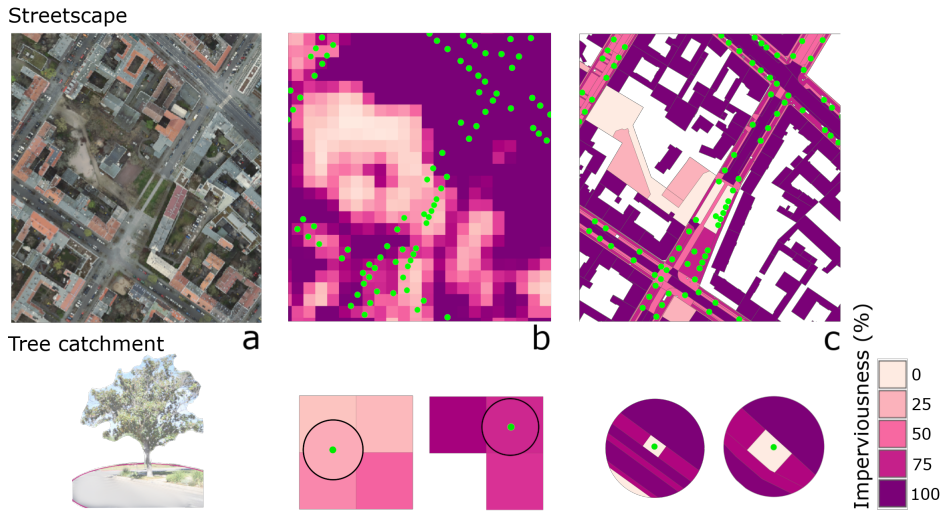

Figure 1: Two samples of imperviousness data on street level and tree catchment level, green dot represent street trees. a: orthophoto of a streetscape and schematic illustration of tree catchment, b: Imperviousness Density 2018 raster product by Copernicus, c: compiled high-resolution polygon dataset of public space, building foot prints and green spaces. Darker colors represent higher imperviousness.

2.3. Imperviousness data

The European satellite-derived data product Imperviousness Density 2018 by Copernicus was used for Berlin to map and analyze imperviousness at the tree catchment scale. It captures the percentage of soil sealing at a resolution of 10 m. The raster values represent the percentage (0-100 %) of each grid cell covered with built infrastructure. Panel b in Figure 1 shows the data for an exemplary streetscape and city block.

2.3.1. Curation of new high-resolution dataset

Furthermore, a new dataset (Willaredt, 2025) was curated from an openly available digital representation of public road space across the city of Berlin

(Senatsverwaltung für Stadtentwicklung und Wohnen Berlin, 2014). The public data were mapped and digitized through a ground survey conducted in 2014 and 2015. The dataset comprises all compartments of the public space, in the following referred to as surface types (e.g., roads, sidewalks, bike lanes) and their respective materials. All layers of surface types, that cover the tree root zone, were selected. Details about included layers are provided in Table A.5 in the Appendix. For 92 % of the area covered by those surface types, pavement materials are specified in the dataset. For six layers the material was not specified. For the surface type bus stop waiting areas, it was possible to detect the pavement material by spatially intersecting with the walkway polygons. To the five remaining surface types (including green area, tree pit, small building structures and cable duct), covering in total 8 % of all mapped catchments, materials of similar surface types were assigned (material codes specified in Table A.5 with corresponding properties listed in Table 2.

For each mapped surface material imperviousness values (i.e., the degree of sealing) and infiltration reduction were matched with the empirical data compiled in the comprehensive review by Timm et al. (2018), summarized in Table 2. Timm et al. (2018) assembled data from studies that quantify the annual hydrological balance around pavement materials under temperate climate. Their results are presented as ranges and for this study the mean values were used. Panel c in Figure 1 illustrates an example of imperviousness data of a typical Berlin's streetscape collected using the new dataset.

Table 2: Ranges of imperviousness (degree of sealing) and annual infiltration reduction observed on different pavement materials, values calculated based on empirical results summarized in (Timm et al., 2018)

Code	**Pavement material**	**Imperviousness** (%)	**Infiltration Reduction** (%)	**Class**
00	Building	100	100	IV
01	Concrete	98-100	91-94	IV
02	Asphalt	98-100	91-94	IV
03	Mosaic Paving	70-95	21-33	II
04	Small Stone Paving	70-95	21-33	II
05	Large Stone Paving	70-95	21-33	II
06	Concrete Paving Stones	70-95	21-33	II
07	Concrete Slabs	95-98	36-47	III
08	Natural Stone Slabs	95-98	36-47	III
09	Large Format Granite Slab	95-98	36-47	III
10	Large Format Concrete Slab	95-98	36-47	III
11	Asphalt Overlay on Paving	98-100	91-94	IV
12	Asphalt Overlay on Concrete	98-100	91-94	IV
13	Stabilized gravel	0	33	I
14	Unsealed (e.g. Soil, substrate)	0	0-2	unpaved
15	Green Area	0	0-2	unpaved

2.3.2. Street trees selection for catchment analysis

For the analysis, only street trees were considered, as they are mostly grown in highly paved settings and are therefore more likely to have constrained water supply (Leisenheimer et al., 2024; Haa, a). The tree inventory of the City of Berlin comprises data on more than 430,000 public street trees (Table A.4). In addition to tree locations, it describes each stem's species identity (genus, species, common name) and morphometric traits (e.g., age, stem circumference, tree height, and crown diameter). Diameter at breast height (DBH) was calculated from the stem circumference assuming a circular stem section. The street tree database was filtered for trees younger than 100 years whose locations intersect with a mapped tree pit or small green area ($< 90\,\mathrm{m}^2$) from the Strassenbefahrung 2014 dataset (Table A.5). The locations could be matched for 33.4 % of the trees. For 82,929 mapped tree pits there was no intersecting tree location in our GIS analysis; probably due to inaccuracies of GPS positioning in cities. To account for misaligned configurations, the intersection was performed using a buffer of 1.5 m around the tree pit to identify the belonging trees. This method recovered 19,733 trees (5.1 %). For those trees, their location was redefined using the centroid of their tree pit. Further, tree pits that contain more than one tree were excluded from this analysis, resulting in a total of 144,182 trees (Figure 2).

A circular buffer in the size of the tree catchment was defined around each tree. The catchment radius was calculated, based on the relationship between the respective tree DBH and maximum root spread as modeled

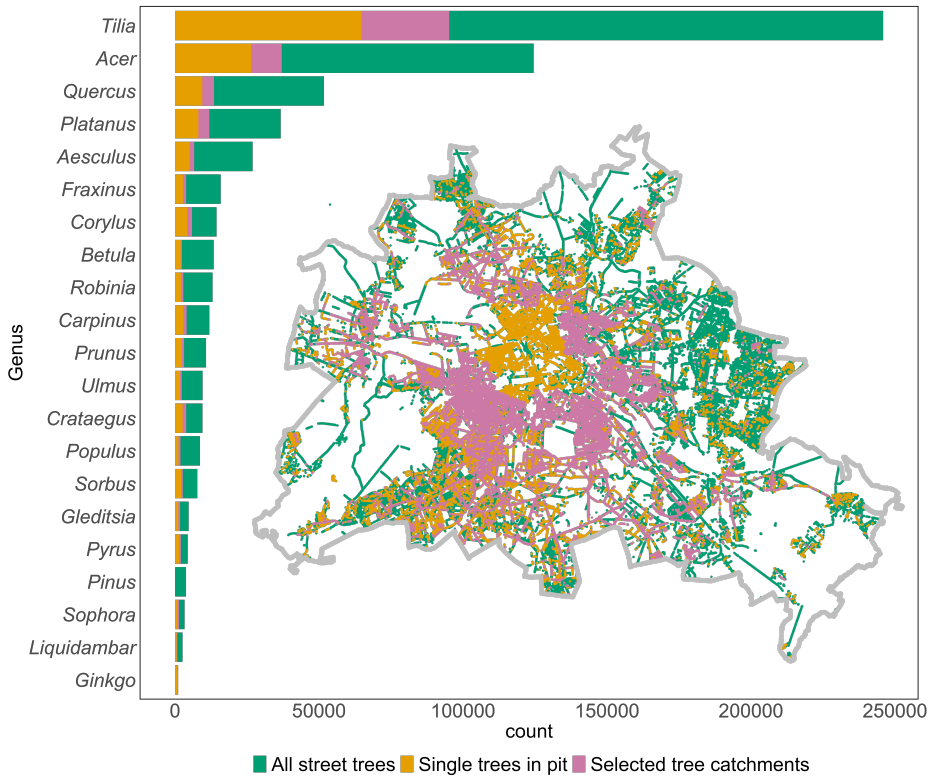

Figure 2: The 20 most commonly planted genera of street trees (> 200 stems) in the city of Berlin. The colors indicate trees that were selected for analyzing their catchment in three iterations 1: selecting street trees of all urban trees, 2: selecting single trees growing in one tree pit and 3: selecting trees with complete catchment datasets (compare Section Appendix A.1)

by (Day et al., 2010) as Equation 1. Panel a in Figure 1 illustrates the delineation of a tree catchment in a schematic way. Every catchment polygon was used to crop the two imperviousness input datasets described above, Figure 1 illustrates examples of both datasets. Following cropping, each polygon dataset was analyzed for completeness comparing the catchment area with the summed areas of the sub-polygons. The differences found were classified according to the type (complete, missing, overlap) and the order of magnitude of the differences (see Section Appendix A.2 for more details). Complete catchments and catchments with missing or overlapping polygons classified as tiny ($< 5\,\%$) were included for the analysis. All catchments located in the Berlin-Mitte district were excluded from the dataset after reviewing their tree pit size distribution. The polygons were uniformly sized and circular, which did not reflect their actual appearance, likely because Berlin-Mitte served as the pilot district for data collection. The final dataset includes catchments for 71,311 trees. Figure 2 shows a map with all street trees, the subset of single trees in individual tree pits, and the final dataset, along with the abundances of the 20 most common genus.

2.4. Analyzing and comparing catchments

2.4.1. Imperviousness

The total imperviousness in each catchment was calculated as the weighted mean of all cropped raster grid cells or polygons using the following equation:

$$Imp_{mean} = \sum A_i \cdot Imp_i \tag{2}$$

where A stands for the area of the cropped grid cell or sub-polygon and *Imp* stands for its respective mean imperviousness value (compare Table 2). The values were rounded to whole numbers, to facilitate the identification of catchments with little to no difference in imperviousness between the two datasets, sub-integer differences were considered negligible. Results describing imperviousness at the tree catchment scale are reported based on the newly curated high-resolution data. The imperviousness is described across the districts as well as the location within the city (central vs. peripheral neighborhoods). The spatial autocorrelation was assessed using Moran's I to test for independence.

2.4.2. Data agreement

The agreement between satellite-derived imperviousness and the high-resolution dataset was quantified and classified (over- and under-estimation) by calculating the difference between satellite-derived data and ground survey–based data and comparing their overall means and distribution. Additionally, Spearman's correlation ρ as well as RMSE and MAE were determined. Due to the presence of spatial autocorrelation in imperviousness, statistical tests assuming independent observations were not applied. Instead, the spatial distribution of the differences was examined visually and with descriptive statistics, in regard to the location of catchments within the

city (central vs. peripheral neighborhood) and administrative boundaries (districts).

2.4.3. Infiltration reduction

The annual mean reduction of infiltration in each catchment was calculated based on the pavement materials specified in the polygon dataset to assess the impact of different pavement layouts. The weighted mean, with respect to areas of each mapped pavement material, was calculated analogously to the mean imperviousness described in Equation 2. For that, the ground survey-based data was merged with the empirical pavement material-specific water balance data (Table 2, (Timm et al., 2018)). The empirical data are based on annual water balance and our approach assumes that all precipitation might eventually reach the tree catchment either via stem-flow or through-fall. It does not consider slopes in the catchments, e.g. resulting from uplifted pavement by roots or topographical slope. To evaluate how well imperviousness approximates infiltration reduction in paved tree catchments, Spearman's correlations between infiltration reduction and both datasets were performed to describe the strength and direction of the relationship. To obtain more detailed insights infiltration reduction values were compared between ten incremental imperviousness classes (10 % intervals) based on the high-resolution data. Further, the largest share of each material class (dominant material class, see Table 2 for classification of pavement materials) covering the tree root zone was calculated for all catchments to

group them accordingly. For each group, the relationship between the size of the share and the infiltration reduction was assessed using regression lines. To analyze the relationship between the hydrological findings and urban form, the catchments were spatially associated to the urban structure dataset of Berlin, describing the urban form on block level (Table A.4). The infiltration reduction as well as proportions of the dominant pavement material class were compared between urban form types of distinct building eras.

In the final step it is demonstrated how this study facilitates the identification of trees with infiltration reduction constraining water supply below transpiration demand during the growing season. The annual transpiration demand for *Tilia* trees, the most abundant genus planted in Berlin, was calculated using a mean daily transpiration rate of middle-aged trees ($87\,\mathrm{L\,d^{-1}}$ reported by Tams et al. (2024)) and scaled by the length of the vegetation period in Germany (221 days (Kaspar et al., 2015)). For each tree (age > 40 years) the difference to the annual potential infiltration based on the annual precipitation recorded for 2024 (553.3 mm (Deutscher Wetterdienst, 2024)) was calculated, mapped and described. Additionally the infiltration reduction in catchments of the 20 most abundant genera planted in Berlin ($n > 200$) are calculated and ranked. All data curation, analysis and visualization was done in R (4.5.0) (R Core Team, 2024). All reported results are presented as means with standard deviations unless otherwise stated.

3. Results

3.1. Imperviousness

The 71,311 analyzed catchments of the street trees in Berlin are severely paved with a mean imperviousness of $79.7 \pm 10.5\,\%$ (SD). Moran's I indicated strong positive spatial autocorrelation of imperviousness in tree catchments (Moran's $I = 0.54, Z = 218.46, p < 0.001$), demonstrating that observations are not spatially independent. Because the data are unevenly distributed along linear street networks, with some trees having only very distant neighbors ($> 1.000\,\mathrm{m}$), the further assessment of clusters using Local Indicators of Spatial Association was not applied in this analysis. Imperviousness in tree catchments is equally high in catchments located in central neighborhoods ($80.4 \pm 9.24\%$) compared to peripheral neighborhoods ($78.5 \pm 12.1\%$) (Figure A.11). The comparison of imperviousness between districts revealed small differences in imperviousness between most districts with overall small differences in mean imperviousness ranging between $76.3 - 81.6\%$ with one exception: the district Marzahn-Hellersdorf with contrastingly low mean imperviousness of 64.7%. Figure A.10 in the Appendix illustrates the respective distributions detailed for each district. The district with the highest mean imperviousness in tree catchments is Tempelhof-Schöneberg.

3.2. Data agreement

For 99% of the studied catchments in Berlin, Germany, satellite-derived imperviousness data did not match imperviousness on the metric scale of sin-

gle urban trees. The mean imperviousness at the tree catchment scale was underestimated in most of the analyzed catchments (n = 41,693, 58.5 %) and overestimated in 28,888 (40.5 %). According to the high-resolution polygon-based dataset assembled from municipal data, the imperviousness resulted to be on average 13.1 % points higher, than detected by satellite data. In 730 catchments the datasets showed agreement (1.02 %). In some cases, the magnitude of disagreement was so large that both datasets showed opposing values for imperviousness, hence the difference at the catchment level was substantial (MAE = 26.3, RMSE = 32.9). Accordingly, the correlation between the values obtained from the two datasets was notably low (Spearman's $\rho = 0.06$). On average, the disagreement between the datasets was greater in underestimated catchments (34 $\pm$21 %) compared to overestimated catchments (16$\pm$12 %).

The graph and map in Figure 3 detail the magnitude of disagreement between the two datasets as well as their spatial distribution across the city. A visual inspection of the spatial distribution revealed that overestimation of imperviousness from satellite data occurs for many tree catchments in the eastern part of Berlin and in the northwest, represented by blue colors. However, the magnitude, represented by color intensity, appears smaller compared to catchments located in central western longitudes. The disagreement in central (n = 38,379), as well as peripheral catchments (n = 32,932) both reflect underestimation with respective means of -10.2 and -16.6 (Figure A.9). A more detailed analysis of disagreement across incremental imperviousness

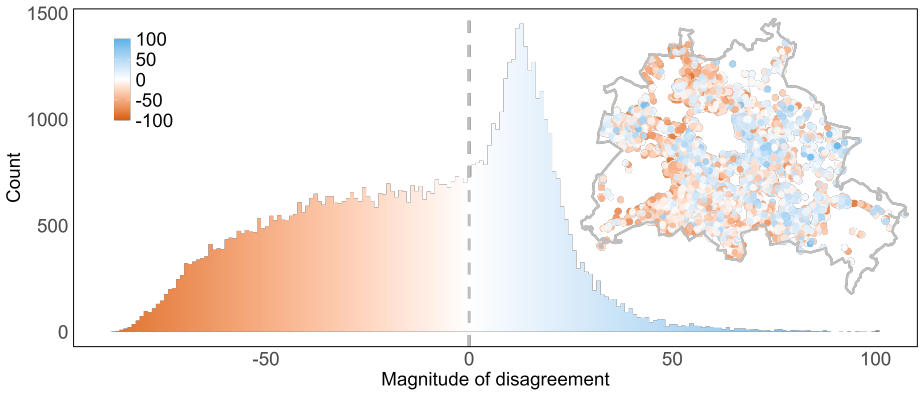

Figure 3: Distribution and magnitude of disagreement between the imperviousness in tree catchments calculated as the difference between satellite-derived (raster) data and ground survey based (polygon) data. Red represents tree catchments with underestimated imperviousness, blue represents overestimated imperviousness, color intensity represents the magnitude of disagreement. The map illustrates spatial distribution of disagreement across the city

ranges shows that the magnitude of overestimation decreases for catchments with imperviousness $>$ 50%, while the magnitude of underestimation increases (Figure A.8).

3.3. Infiltration reduction

The presence of pavement in street tree catchments can severely reduce the mean annual water supply from stormwater. In the analyzed 71,311 catchments, pavements decrease infiltration by 45.9($\pm$12.8)%. Infiltration reduction is strongly correlated with polygon-based imperviousness (Spearman's $\rho = 0.74$, $p < 0.001$). However, grouping the catchments by incremental imperviousness reveals that the infiltration reduction exhibits considerable variability (Figure 4 a) in catchments with high imperviousness. This indicates that infiltration reduction might not be accurately captured

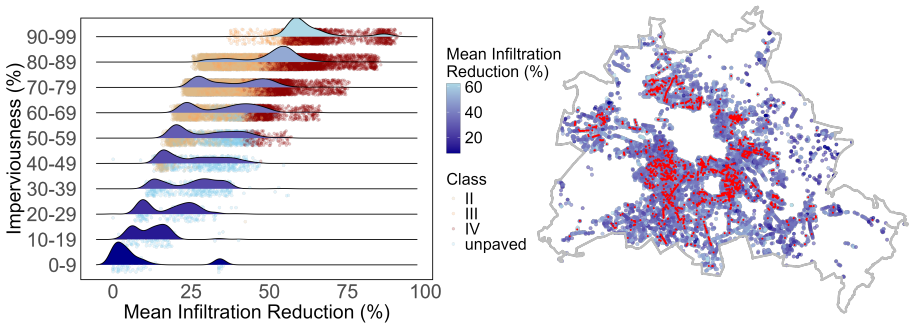

Figure 4: Diagram illustrating the distribution of infiltration reduction identified for similar levels of imperviousness in paved tree catchments, lighter colors represent less infiltration. b Map illustrating the spatial distribution of catchments with reduced infiltration across the city of Berlin. Red dots mark *Tilia* trees with insufficient annual infiltration to cover transpiration demand.

at the upper end of the imperviousness range. The Spearman's rank correlation reveals no relationship between infiltration reduction and raster-based imperviousness ($\rho = -0.006$, $p < 0.001$).

The mean infiltration reduction across catchments exhibits a bimodal distribution, in contrast to the more uniform and skewed distribution of mean imperviousness (see Figure A.10). When catchments are grouped by the material covering the largest surface area, distinct clusters emerge. Figure 5 visualizes the bimodal distribution and the respective groups, classified by the largest share of pavement material covering the tree catchment. Table 3 summarizes the infiltration reduction for each group. These differences align with separate infiltration-reduction regressions. The data exhibit four distinct regression patterns for each dominant material class (Figure 5 b). Catchments with dominant material materials of Class IV show positive correlation ($R = 0.54$) between the size of the share and the infiltration reduc-

tion, while increasing shares of material of Class III, Class II and unpaved show negative relationships with weaker correlations. Because all analyzed catchments represent street tree environments, pavement is present in most cases, with unpaved surfaces rarely dominating (4% of cases, see Table 3). On average, they consist of eight different materials (Figure A.12). Thus, higher shares of Class III and II materials primarily indicate a substitution of Class IV surfaces, leading to lower infiltration reduction. Moreover, the relationship between catchment size and infiltration reduction is comparable across all material classes (Figure A.13), suggesting that catchment area does not bias this pattern.

Table 3: Summary statistics of infiltration reduction in tree catchments grouped by largest share of pavement material class present (dominant material class). Note that no catchment has pavement material of Class I detected as the dominant material class.

Material class	**n**	**Infiltration reduction**		
		Mean ± SD	**Min**	**Max**
Unpaved	2,854	29.9 ± 11.1	0.0	56.1
II	30,986	36.9 ± 9.77	13.1	59.4
III	6,390	46.5 ± 8.66	22.1	65.1
IV	31,081	56.2 ± 6.66	40	92

Unpaved: Soil, Substrate, Green Area; Class II: Mosaic, Small and Large Stone Paving, Concrete Paving Stones, Class III: Concrete and Natural Stone Slabs, Large Format Granite and Concrete Slabs.

Hence, for trees growing in catchments that are covered with 75 % Asphalt, the water supply from precipitation could on average potentially be increased by 56 % if it would be removed or approximately 30 % if it was replaced with a material belonging to the Class II (example materials listed

in Table 2).

Comparing the distribution of infiltration reduction in catchments adjacent to blocks of distinct urban structure types (Figure A.14) reveals that mean infiltration reduction differs little even across contrasting urban forms. For instance, dense historic block developments (1870s–1918) and large post-war housing estates (1960s–1990s) show mean infiltration reductions of 44.2% and 50.1% respectively. The mean infiltration reduction in catchments adjacent to the city squares or promenades, stand out: they show the lowest mean infiltration reduction of 33.9%. Figure A.15 reinforces the role of dominant material classes in catchments: the proportion of the dominant pavement material in the catchment remains the primary driver of infiltration reduction, and this proportion varies little across most urban structure types.

The three most abundant tree genera in Berlin are *Tilia*, *Acer* and *Quercus*, they have potential reduction of infiltration of 46.3±12.7%, 46.1±13.2%, 47.9 ± 11.3%, respectively. The comparison of the potentially infiltrated amount of water in the catchments of mature *Tilia* trees with the cumulatively transpired amount of water during the vegetation period identifies 3,361 trees with a possible theoretical water deficit based on the annual precipitation recorded for the year 2024. This accounts to $\sim$ 19.8 % of *Tilias* in the analyzed dataset that are older than 40 years. Their location is highlighted as red dots in Figure 4. *Ginkgo*, *Betula* and *Robinia* trees are planted in catchment with layouts causing the highest reduction of storm-water infiltration. Figure 6 ranks tree genera according to the magnitude of infiltration

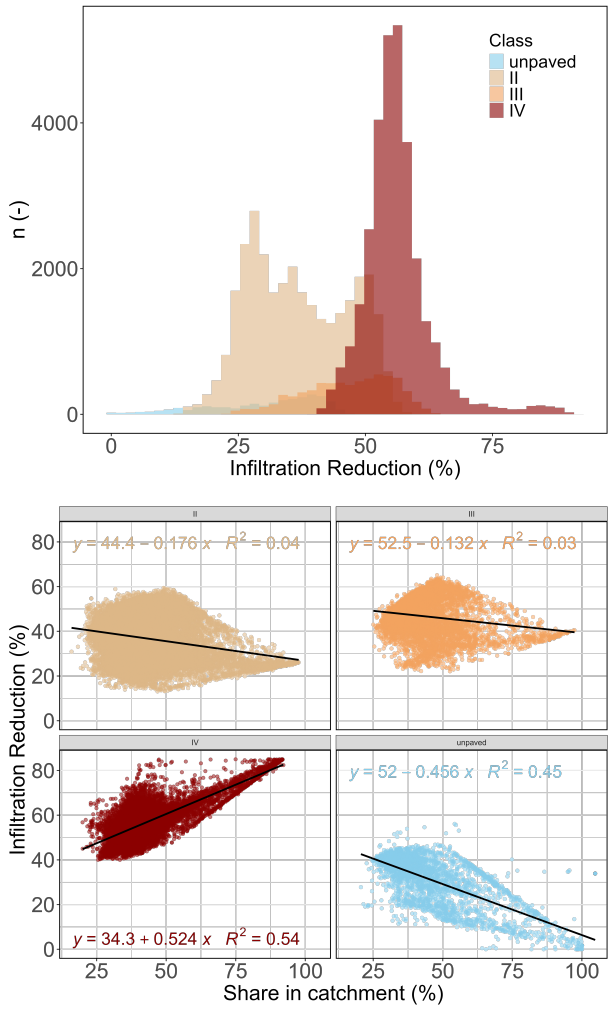

Figure 5: Upper panel: Distribution of weighted mean infiltration reduction across 71,311 analyzed catchments. Colors represent the class of the dominant material share identified for the catchment. Lower panel: Relationship between the relative size of the dominant material share in (%) and the weighted mean reduction of infiltration in the entire catchment. Note that no catchment has pavement material of Class I detected as the dominant material class.

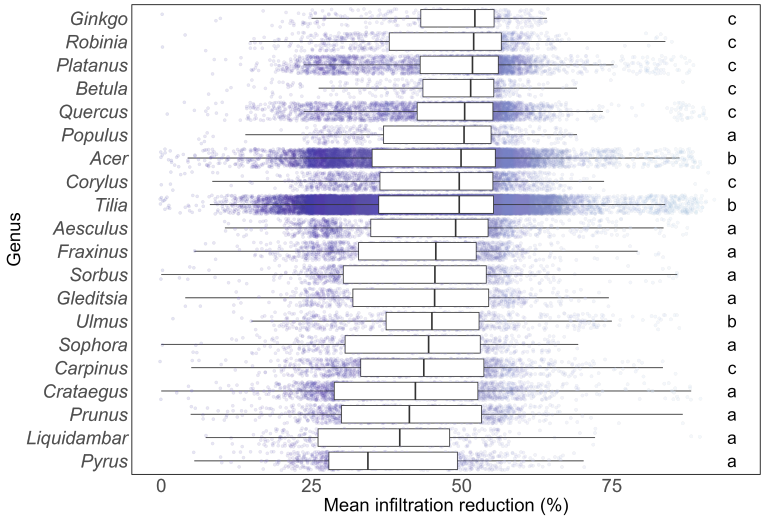

Figure 6: Ranking of infiltration reduction in catchments of genera with stem numbers > 200. Each dot being a street tree catchment grouped by the planted genus. Lighter colors represent less infiltration of stormwater. Letters indicate significant differences ($p < 0.05$) in storm water infiltration reduction between genera.

reduction caused by pavement layout in their catchments.

4. Discussion

4.1. Limitations of satellite-derived imperviousness at tree scale

Satellite-derived imperviousness data do not accurately reflect imperviousness on the metric scale of single street trees. In general, the imperviousness is underestimated which coincides with findings from (Techapinyawat et al., 2024) who found underestimation even for high-resolution aerial imagery. However, as the data exhibit significant spatial autocorrelation, the compared catchments cannot be treated as fully independent observations, and the uncertainty around the reported error metrics (MAE, RMSE) and

correlation coefficients (Spearman's ρ) is therefore likely underestimated and should be interpreted accordingly. The main reason for underestimation may be the obstruction of the ground by tree canopies, even during the leaf-off period in deciduous trees. The availability of tree canopy cover data combined with algorithms that extrapolate the extent of an impervious surface based on logical and geometric constraints, can improve the accuracy of remotely sensed data (Techapinyawat et al., 2024).

The significant spatial auto-correlation reflects that street trees are arranged along streets with similar properties. However, in contrast to imperviousness on the city scale described in Haa (b), imperviousness in the tree catchment scale does not decline along the urban-rural gradient. Further, the administrative boundaries of districts in Berlin seem to be too large to reflect the spatial variability found in this study. One exception is the district Marzahn-Hellersdorf situated in the North-East of Berlin. Large parts of it were mainly developed after the 1970s and therefore they might more homogeneously reflect the urban design of residential areas in the German Democratic Republic (GDR) (Wellmann et al., 2020). In parts of Berlin, that were developed during the GDR street trees are planted in less paved environments along wider street scapes (Magistral) with larger spatially connected tree growth elements. In contrast, the district presenting the highest imperviousness in tree catchments, Tempelhof-Schoeneberg, is coined by the dense development during the historical period of rapid industrial growth in Germany (Gründerzeit). This indicates that imperviousness at the tree

catchment scale might be more influenced by urban design instead of the classic urban-rural gradient. The large difference identified between street tree scale imperviousness and neighborhood scale (compare Table 1), highlights the importance of scale in analyzing imperviousness, for instance when identifying priority regions for climate adaptation strategies. However, the sample size for analyzed trees in the eastern longitudes is comparably small, likely because of the exclusion of tree pits with more than one tree, which are common in the previously described larger tree pits in the eastern districts in Berlin.

4.2. Pavement material better explains infiltration reduction

The infiltration reduction is reflected by imperviousness at the tree catchment level to a limited extent. Despite the positive corelation between both characteristics, the weighted mean imperviousness at the catchment scale can reflect distinct underlying pavement layouts. This is particularly evident in the bimodal distributions of catchment level infiltration reduction across incremental steps of imperviousness (Figure 4). The fragmentation of surfaces e.g., by the joints between single paving stones, allows substantial infiltration (Timm et al., 2018). Therefore similar degrees of imperviousness at the tree catchment level can still lead to distinctly different infiltration reductions, which rather reflect the dominant pavement material present in each catchment (Figure 5). The intuitive decrease of infiltration on pavement materials with less permeability is in concordance with results from an experimental

set up performed by Fini et al. (2022), who report significantly lower soil moisture measured under impermeable pavement.

Thus, imperviousness data that capture the level of detail of pavement materials are required to reliably estimate the impact of pavement on tree water supply. Such datasets might become more readily available in the future as cities develop digital urban twins initiatives. Additionally, the emerging AI-supported classification of street level imagery (Kapp et al., 2024), predominantly for road quality assessment and urban tree species (Velasquez-Camacho et al., 2025), could soon replace costly ground surveys to obtain similarly high detailed datasets for urban tree planting sites. The high-resolution data compiled for this study could serve as proof-of-concept and validation of such technological developments. The grouping of tree catchments in accordance with the pavement materials classes introduced by Timm et al. (2018), helps to estimate the impact de-sealing or the replacement of the dominant pavement material could have. This provides valuable guidance to decision makers regarding the choice of materials or the impact of de-sealing as a means of climate adaptation to promote tree longevity (Just et al., 2018).

4.3. Infiltration reduction limits water supply for street trees

According to Smith et al. (2023), precipitation is considered a major source of water supply for urban trees in humid climate, even in paved environments. However, depending on annual climatic conditions and under a

changing climate, water supply for many trees might be compromised by the presence of pavements. This was demonstrated in the case of *Tilia*, the most abundantly planted genus in Berlin, where trees were identified in catchments in which reduced infiltration might have left the tree water supply below transpiration demand during the growing season. Block-level attributes such as building era or urban structure type tested in this analysis cannot indicate high infiltration reduction at the individual tree level, since the pavement materials on streets between blocks, do not necessarily reflect the density of the adjacent urban structure type. Through the presented approach, more efficient water management strategies could be designed and implemented, particularly if trees that would benefit most from retrofitting of pavement layouts in their catchments could be pinpointed.

In the semi-arid climate of Los Angeles Bijoor et al. (2011) found that urban trees are largely dependent on irrigation water taken up from shallow soil depth as few trees can access groundwater. In those cases, the pavement could be designed to support retaining soil water resources by decreasing evaporation. However, the accumulation of soil moisture in shallow depth under pavement (Schaffitel et al., 2020) also known to trigger shallow tree root growth, which can cause other challenges. The material specific infiltration properties used in this study were annual mean values from empirically collected ranges (see Table 2). The variability, is therefore likely higher. Additionally, precipitation patterns determine infiltration processes around pavement significantly (Nehls et al., 2011; Haacke and Paton, 2023).

Whereas previous studies had to rely on environmental properties derived at coarser spatial scales due to the lack of high-resolution data (Pattnaik et al., 2024; Franceschi et al., 2023; Dahlhausen et al., 2017), this study advances the field using data on the level of individual trees, allowing for a more precise evaluation of the impact of pavement at the scale of individual trees. Finally, this study highlights pavement as an important factor to consider in studies relating climatic conditions, especially precipitation, in urban areas to tree growth, as its presence can change the available resource significantly.

4.4. Limitations and future directions

The soil volume explored by urban tree roots remains literally in the dark. The assumptions used in this study may not represent the catchments for many trees especially where build structures, like basements hinder root growth (Lüttge and Buckeridge, 2020; Mullaney et al., 2015) or underground infrastructure such as pipes may attract roots (Oss). Where trees grow in trenches or multiple trees are planted in larger green areas in street settings, the roots may interact. This limitation of the study points to a research gap in urban forestry which could be addressed with further development of ground penetrating radar measurements on tree roots (Nichols et al., 2017). More precise knowledge of individual root spread could lead to different catchment delineations than applied here, and consequently to different infiltration reduction estimates. However, the more constrained a root system is by sur-

rounding urban infrastructure, the greater the likelihood that the tree suffers from water deficit. Other important factors influencing infiltration, like slope or uplifting of pavement (Mullaney et al., 2015) by roots can either increase run off or cause small depressions that potentially serve as temporal storage and add to tree water supply (Timm et al., 2018).

The study of interception was out of the scope of this paper. However it will reduce the amount of precipitation reaching the pavement under the tree canopy and needs to be included when assessing the water supply for trees. Interception will be different, depending on species specific traits (Dowtin et al., 2023).

The hydrological classification of pavement materials used in this study (Timm et al., 2018) is limited to reflecting only the annual water balance and neglects the role that precipitation duration and characteristics (Nehls et al., 2011) play in the hydrological balance around different pavement types. Furthermore, the data reflect the hydrological balance in temperate humid climate only and the infiltration reduction may differ in other climate zones and in future climate. Advances in distinguishing the hydrological behavior of pavement materials, with respect to atmospheric forcing, could be derived from observational, like the dataset presented by Schaffitel et al. (2020). They provide time series of water contents (hourly resolution), and infiltration under 18 different pavement materials. Such observations can be used to identify highly relevant phenomena for urban trees such as temporary saturation, which implies a lack of oxygen for root respiration and can lead to

reduced root production (Viswanathan et al., 2011).

The new data presented here can leverage large-scale urban forestry field studies, including dendrochronology, along water supply gradients for advancing the knowledge about the relationship between growth, water limitation and stress resilience of trees. Specifically, investigating the hydraulic transport systems of urban trees developed in water limited conditions (Grote et al., 2016) promises advances in identifying urban trees at risk and could thus support urban tree management. The city wide scale of the presented dataset could be especially interesting for analyzing remotely sensed indicators of tree water stress (e.g. using NDVI) (Leisenheimer et al., 2024; Miller et al., 2020). In addition such data can refine model approaches for prediction of potential drought stress of trees like in (Kluge and Kirmaier, 2024), which include pavement layout as an input factor.

Beyond academic contributions, this study also has practical relevance. The results may inform ongoing climate adaptation strategies, such as pavement removal or replacement to increase tree pit sizes e.g. in the district of Berlin-Kreuzberg (Bezirksamt Friedrichshain-Kreuzberg, 2024) and provide a foundation for evaluating current regulations and guidelines for tree planting in urban environments. The high resolution and the evaluation for each specific tree catchment enable clear rankings and decisions for urban planners or foresters, which makes the results very valuable.

Given the availability of pavement material data and tree inventory data that includes DBH, this study can be easily repeated in other cities in tem-

perate climate. However, while remotely sensed imperviousness data is commonly available it lacks the material-level resolution required for this analysis. For this approach to be widely adopted by policymakers and practitioners, high-resolution pavement material data would first need to be made available. Promising computer vision based approaches, like CitySurfaces (Hosseini et al., 2022), may facilitate such data acquisition in the future.

A further limitation to the transferability of these findings is that the pavement material infiltration properties applied in this study were empirically determined under temperate climate conditions and may not be representative of other climatic contexts. Addressing this would either require the assembly of climate-specific material property datasets, or the development of a more mechanistic understanding of infiltration processes that accounts for local precipitation patterns and vapor pressure deficit.

5. Conclusion

High-resolution imperviousness data that captures pavement materials can advance the knowledge about water availability for street trees. This study leverages public urban data for mapping imperviousness in the near vicinity of street trees, the tree catchment, to determine the extent to which the presence of pavement reduces the water supply from stormwater infiltration. It presents a newly curated dataset on imperviousness in tree catchments that captures the level of detail of pavement materials and merges it with their hydrological properties. The study quantifies the limitations

of satellite-derived imperviousness data for analysis at the tree catchment level comparing the catchments of 71,311 street trees. Satellite-derived data mostly underestimates imperviousness at the tree catchment scale. Further, the study highlights that imperviousness at the tree catchment scale does not accurately estimates the reduction of infiltration caused by the presence of pavement as it cannot capture the variability of pavement materials found in tree catchments. Instead, the results demonstrate that for analyzing the impact pavement has on street tree water supply it is necessary to consider the main pavement materials and their respective hydrologic properties. The results show that the presence of pavement reduces the potential mean annual water supply from stormwater on average by 45.9 %. This result opens the question on whether street trees grown in paved environments experience a modified climatic water regime that differs from the regional climate in their respective geographic location. A better mechanistic understanding on the water balance of paved soils would enhance the transferability of this study to cities in other climate zones. The practical relevance of the work was demonstrated by the identification of *Tilia* trees in catchments where infiltration reduction caused by pavement might compromise the water supply necessary to meet the transpiration demand during the vegetation period. Such investigations, including other tree species and climate predictions could inform climate adaptation strategies in urban planning and tree water management.

6. CRediT authorship contribution statement

M.W. Writing – original draft, Writing – review & editing, Visualization, Methodology, Funding acquisition, Data curation, Formal analysis, Conceptualization. **A.O.** Writing – review & editing, Visualization, Methodology, Conceptualization, Discussion, Supervision. **D.H.** Writing – review & editing, Methodology, Conceptualization, Discussion.

7. Declaration of competing interest

The authors declare that they have no known competing interests.

8. Acknowledgments

This project received funding for M.W. by the Deutsche Forschungsgemeinschaft (DFG, German Research Foundation - 529031514) and by a Hatch Project (CA-D-PLS-2735-H) to A.O.. D.H. is funded by the NaturaConnect (Designing a resilient and coherent Trans-European Network for Nature and People) Horizon 2020 project (contract no. 101060429). M.W. thanks Elizeth Cinto Mejía, Luisa Fernanda Velásquez Camacho and Pooja Singh for their feedback on many aspects of this work and for their warm academic companionship. Further, M.W. thanks Sasha Osorio for her support as a writing consultant at the UC Davis Writing Center and Björn Kluge for clarifications about hydrologic classification of pavement materials.

9. Data availability

The data used for this work is published in (Willaredt, 2025). It can be downloaded from `https://doi.org/10.5281/zenodo.17316494` and explored in an interactive RShiny App:

`https://mowill.shinyapps.io/TreeCatchmentDataVisualization/`

10. Declaration of generative AI and AI-assisted technologies in the manuscript preparation process

During the preparation of this work, the author(s) used ChatGPT (OpenAI, 2025) and Claude (Anthropic, 2025) in order to improve the clarity of the manuscript text and to assist in refining R code during data processing. After using these tools, the authors reviewed and edited the content as needed and take full responsibility for the content of the published article.

References

, a .

, b .

, .

Amt für Statistik Berlin-Brandenburg, 2025. Einwohnerregisterstatistik Berlin 31. Dezember 2024: Bestand - LOR-Planungsräume. Statistischer Bericht A I 16 – hj 2/24. Amt für Statistik Berlin-Brandenburg. Steinstraße 104-106, 14480 Potsdam. URL: `https://www.`

675 statistik-berlin-brandenburg.de. bezirke und Lebensweltlich orien-
676 tierte Räume (LOR-Planungsräume) von Berlin.

677 Bezirksamt Friedrichshain-Kreuzberg, 2024. Ruhlsdorfer straße
678 – platz für gesunde bäume. https://www.berlin.de/
679 ba-friedrichshain-kreuzberg/politik-und-verwaltung/aemter/
680 strassen-und-gruenflaechenamt/strassen/artikel.1471667.php.
681 Press release / web article, Berlin.de.

682 Bijoor, N.S., McCarthy, H.R., Zhang, D., Pataki, D.E., 2011. Water sources
683 of urban trees in the los angeles metropolitan area. Urban Ecosystems 15,
684 195–214. doi:10.1007/s11252-011-0196-1.

685 Browning, M., Locke, D., Konijnendijk, C., Labib, S., Rigolon, A., Yeager,
686 R., Bardhan, M., Berland, A., Dadvand, P., Helbich, M., Li, F., Li, H.,
687 James, P., Klompmaker, J., Reuben, A., Roman, L., Tsai, W.L., Patwary,
688 M., O'Neil-Dunne, J., Ossola, A., Wang, R., Yang, B., Yi, L., Zhang, J.,
689 Nieuwenhuijsen, M., 2024. Measuring the 3-30-300 rule to help cities meet
690 nature access thresholds. Science of The Total Environment 907, 167739.
691 doi:https://doi.org/10.1016/j.scitotenv.2023.167739.

692 Cinto Mejía, E., Ossola, A., Willaredt, M., Lippey, M., Roper, O.,
693 Chaturvedi, S., Youngsteadt, E., Meineke, E., 2025. Urban surface tem-
694 perature and soil compaction, but not precipitation, predict tree water
695 hydration status across three cities. Under Review.

City of Melbourne, 2016. Road segments with surface type. URL: https://data.melbourne.vic.gov.au/datasets/road-segments-with-surface-type. dataset Identifier: road-segments-with-surface-type.

Croeser, T., Sharma, R., Weisser, W.W., Bekessy, S.A., 2024. Acute canopy deficits in global cities exposed by the 3-30-300 benchmark for urban nature. Nature Communications 15. doi:https://doi.org/10.1038/s41467-024-53402-2.

Dahlhausen, J., Rötzer, T., Biber, P., Uhl, E., Pretzsch, H., 2017. Urban climate modifies tree growth in berlin. International Journal of Biometeorology 62, 795–808. doi:10.1007/s00484-017-1481-3.

Day, S.D., Wiseman, P.E., Dickinson, S.B., Harris, J.R., 2010. Contemporary concepts of root system architecture of urban trees. Arboriculture & Urban Forestry (AUF) 36, 149–159.

Deutscher Wetterdienst, 2024. Jahreswerte der niederschlagshöhe für station 00433. Climate Data Center (CDC). URL: https://opendata.dwd.de/climate_environment/CDC/. [dataset] Zeitraum: 2020-01-01 bis 2024-12-31.

Dowtin, A.L., Cregg, B.C., Nowak, D.J., Levia, D.F., 2023. Towards optimized runoff reduction by urban tree cover: A review of key physical tree traits, site conditions, and management strategies. Landscape and Urban

717 Planning 239, 104849. doi:https://doi.org/10.1016/j.landurbplan.
718 2023.104849.

719 Esperon-Rodriguez, M., Gallagher, R.V., Russo, A., Power, S.A., Calaza-
720 Martínez, P., Capela Lourenço, T., Cariñanos, P., Eleuterio, A.A., Guo, Z.,
721 Lee, G., Masselot, P., Mcdonald, R.I., Messier, C., Ordoñez, C., Parpanchi,
722 M., Schifanella, R., Shackleton, C., Sharmin, M., Solfjeld, I., St-Denis, A.,
723 Svenning, J.C., Torres-Martinez, M.M., Wiström, B., Yan, P., Yang, J.,
724 Tjoelker, M.G., 2025. Global trends in urban forest irrigation: Environ-
725 mental influences, challenges and opportunities for sustainable practices
726 across 109 cities worldwide. Sustainable Cities and Society 130, 106510.
727 doi:10.1016/j.scs.2025.106510.

728 European Environment Agency, European Environment Agency,
729 2020. Imperviousness density 2018 (raster 100 m), eu-
730 rope, 3-yearly, aug. 2020. doi:https://doi.org/10.2909/
731 524fa72f-61d7-4364-801e-3e271d7b10bc.

732 Fini, A., Frangi, P., Comin, S., Vigevani, I., Rettori, A.A., Brunetti, C.,
733 Moura, B.B., Ferrini, F., 2022. Effects of pavements on established ur-
734 ban trees: Growth, physiology, ecosystem services and disservices. Land-
735 scape and Urban Planning 226, 104501. doi:10.1016/j.landurbplan.
736 2022.104501.

737 Franceschi, E., Moser-Reischl, A., Honold, M., Rahman, M.A., Pretzsch,
738 H., Pauleit, S., Rötzer, T., 2023. Urban environment, drought events and

climate change strongly affect the growth of common urban tree species in a temperate city. Urban Forestry & Urban Greening 88, 128083. doi:https://doi.org/10.1016/j.ufug.2023.128083.

Gillner, S., Bräuning, A., Roloff, A., 2014. Dendrochronological analysis of urban trees: climatic response and impact of drought on frequently used tree species. Trees 28, 1079–1093. doi:10.1007/s00468-014-1019-9.

Grabosky, J., Bassuk, N., 1995. A new urban tree soil to safely increase rooting volumes under sidewalks. Journal of Arboriculture 21, 187–187.

Gracias, J.S., Parnell, G.S., Specking, E., Pohl, E.A., Buchanan, R., 2023. Smart cities—a structured literature review. Smart Cities 6, 1719–1743. doi:https://doi.org/10.3390/smartcities6040080.

Grote, R., Samson, R., Alonso, R., Amorim, J.H., Cariñanos, P., Churkina, G., Fares, S., Thiec, D.L., Niinemets, U., Mikkelsen, T.N., Paoletti, E., Tiwary, A., Calfapietra, C., 2016. Functional traits of urban trees: air pollution mitigation potential. Frontiers in Ecology and the Environment 14, 543–550. doi:10.1002/fee.1426.

Haacke, N., Paton, E., 2023. Impact-based classification of extreme rainfall events using a simplified overland flow model. Urban Water Journal 20, 330–340. doi:https://doi.org/10.1080/1573062X.2022.2164731.

Hosseini, M., Miranda, F., Lin, J., Silva, C.T., 2022. Citysurfaces: City-scale semantic segmentation of sidewalk materials. Sustainable

760 Cities and Society 79, 103630. URL: https://www.sciencedirect.
761 com/science/article/pii/S2210670721008933, doi:https://doi.org/
762 10.1016/j.scs.2021.103630.

763 Huang, X., Yang, J., Wang, W., Liu, Z., 2022. Mapping 10 m global imper-
764 vious surface area (gisa 10m) using multi-source geospatial data. Earth
765 System Science Data 14, 3649–3672. doi:10.5194/essd-14-3649-2022.

766 Just, M.G., Frank, S.D., Dale, A.G., 2018. Impervious surface thresholds for
767 urban tree site selection. Urban Forestry & Urban Greening 34, 141–146.
768 doi:10.1016/j.ufug.2018.06.008.

769 Kapp, A., Hoffmann, E., Weigmann, E., Mihaljević, H., 2024. SurfaceAI:
770 Automated creation of cohesive road surface quality datasets based on open
771 street-level imagery. doi:https://doi.org/10.1145/3681780.3697277.

772 Kaspar, F., Zimmermann, K., Polte-Rudolf, C., 2015. An overview of the
773 phenological observation network and the phenological database of ger-
774 many's national meteorological service (deutscher wetterdienst). Advances
775 in Science and Research 11, 93–99. doi:10.5194/asr-11-93-2014.

776 Kjelgren, R.K.and Clark, J., 1993. Growth and water relations of liquidambar
777 styraciflua l. in an urban park and plaza. Trees 7. doi:https://doi.org/
778 10.1007/BF00202073.

779 Kluge, B., Kirmaier, M., 2024. Urban trees left high and dry – modelling
780 urban trees´ water supply and evapotranspiration under drought. En-

781 vironmental Research Communications URL: http://iopscience.iop.
782 org/article/10.1088/2515-7620/ad7dda.

783 Leisenheimer, L., Wellmann, T., Jänicke, C., Haase, D., 2024. Monitor-
784 ing drought impacts on street trees using remote sensing - disentangling
785 temporal and species-specific response patterns with sentinel-2 imagery.
786 Ecological Informatics 82, 102659. doi:10.1016/j.ecoinf.2024.102659.

787 Lüttge, U., Buckeridge, M., 2020. Trees: structure and function and the chal-
788 lenges of urbanization. Trees 37, 9–16. doi:10.1007/s00468-020-01964-1.

789 Marchin, R.M., Backes, D., Ossola, A., Leishman, M.R., Tjoelker, M.G.,
790 Ellsworth, D.S., 2021. Extreme heat increases stomatal conductance and
791 drought-induced mortality risk in vulnerable plant species. Global Change
792 Biology 28, 1133–1146. doi:https://doi.org/10.1111/gcb.15976.

793 Miller, D.L., Alonzo, M., Roberts, D.A., Tague, C.L., McFadden, J.P., 2020.
794 Drought response of urban trees and turfgrass using airborne imaging
795 spectroscopy. Remote Sensing of Environment 240, 111646. doi:https:
796 //doi.org/10.1016/j.rse.2020.111646.

797 Moser, A., Rahman, M.A., Pretzsch, H., Pauleit, S., Rötzer, T., 2016. Inter-
798 and intraannual growth patterns of urban small-leaved lime (tilia cor-
799 data mill.) at two public squares with contrasting microclimatic condi-
800 tions. International Journal of Biometeorology 61, 1095–1107. doi:10.
801 1007/s00484-016-1290-0.

Moser-Reischl, A., Rahman, M.A., Pauleit, S., Pretzsch, H., Rötzer, T., 2019. Growth patterns and effects of urban micro-climate on two physiologically contrasting urban tree species. Landscape and Urban Planning 183, 88–99. doi:10.1016/j.landurbplan.2018.11.004.

de la Mota Daniel, F.J., Day, S.D., Owen, J.S., Stewart, R.D., Steele, M.K., Sridhar, V., 2018. Porous-permeable pavements promote growth and establishment and modify root depth distribution of platanus x acerifolia (aiton) willd. in simulated urban tree pits. Urban Forestry & Urban Greening 33, 27–36. doi:https://doi.org/10.1016/j.ufug.2018.05.003.

Mullaney, J., Lucke, T., Trueman, S.J., 2015. A review of benefits and challenges in growing street trees in paved urban environments. Landscape and Urban Planning 134, 157–166. doi:https://doi.org/10.1016/j.landurbplan.2014.10.013.

National Oceanic and Atmospheric Administration, Office for Coastal Management, 2025. 2021 noaa c-cap version 2 impervious cover: California. www.coast.noaa.gov/htdata/raster1/landcover/bulkdownload/hires/. Accessed: March 2025.

Nehls, T., Nam Rim, Y., Wessolek, G., 2011. Technical note on measuring run-off dynamics from pavements using a new device: the weighable tipping bucket. Hydrology and Earth System Sciences 15, 1379–1386. doi:10.5194/hess-15-1379-2011.

Nichols, P., McCallum, A., Lucke, T., 2017. Using ground penetrating radar to locate and categorise tree roots under urban pavements. Urban Forestry Urban Greening 27, 9–14. URL: https://www.sciencedirect.com/science/article/pii/S1618866716303302, doi:https://doi.org/10.1016/j.ufug.2017.06.019.

Pattnaik, N., Honold, M., Franceschi, E., Moser-Reischl, A., Rötzer, T., Pretzsch, H., Pauleit, S., Rahman, M.A., 2024. Growth and cooling potential of urban trees across different levels of imperviousness. Journal of Environmental Management 361, 121242. doi:https://doi.org/10.1016/j.jenvman.2024.121242.

R Core Team, 2024. R: A Language and Environment for Statistical Computing. R Foundation for Statistical Computing. Vienna, Austria. URL: https://www.R-project.org/.

Rissanen, K., Vitali, V., Kneeshaw, D., Paquette, A., 2025. Vessel anatomy of urban celtis occidentalis trees varies to favour safety or efficiency depending on site conditions. Trees 39. doi:https://doi.org/10.1007/s00468-025-02603-3.

Rosenberger, L., Leandro, J., Helmreich, B., 2025. Providing sufficient water for urban trees with limited root space during drought: Modeling of irrigation scenarios in a temperate climate. Urban Forestry & Urban Greening 104, 128670. doi:https://doi.org/10.1016/j.ufug.2025.128670.

Rosenberger, L., Leandro, J., Wood, R., Rötzer, T., Helmreich, B., 2024. Influence of age, soil volume, and climate change on water availability at urban tree sites. Sustainable Cities and Society 113, 105680. doi:https://doi.org/10.1016/j.scs.2024.105680.

Sand, E., Konarska, J., Howe, A.W., Andersson-Sköld, Y., Moldan, F., Pleijel, H., Uddling, J., 2018. Effects of ground surface permeability on the growth of urban linden trees. Urban Ecosystems 21, 691–696. doi:https://doi.org/10.1007/s11252-018-0750-1.

Savi, T., Bertuzzi, S., Branca, S., Tretiach, M., Nardini, A., 2014. Drought-induced xylem cavitation and hydraulic deterioration: risk factors for urban trees under climate change? New Phytologist 205, 1106–1116. doi:https://doi.org/10.1111/nph.13112.

Scalenghe, R., Marsan, F.A., 2009. The anthropogenic sealing of soils in urban areas. Landscape and Urban Planning 90, 1–10. doi:https://doi.org/10.1016/j.landurbplan.2008.10.011.

Schaffitel, A., Schuetz, T., Weiler, M., 2020. A distributed soil moisture, temperature and infiltrometer dataset for permeable pavements and green spaces. Earth System Science Data 12, 501–517. doi:https://doi.org/10.5194/essd-12-501-2020.

Senatsverwaltung für Mobilität, Verkehr, Klimaschutz und Umwelt Berlin, 2024a. Baumbestand berlin. Geoportal berlin. URL: https://

daten.berlin.de/datensaetze/baumbestand-berlin-wms-52e6ddaa. [dataset].

Senatsverwaltung für Mobilität, Verkehr, Klimaschutz und Umwelt Berlin, 2024b. Grünanlagenbestand berlin (einschließlich der öffentlichen spielplätze). Geoportal Berlin. [dataset].

Senatsverwaltung für Stadtentwicklung, Bauen und Wohnen Berlin, 2022. Versiegelung 2021 (umweltatlas). URL: https://www.berlin.de/umweltatlas/boden/versiegelung/2021/zusammenfassung/. [dataset].

Senatsverwaltung für Stadtentwicklung, Bauen und Wohnen Berlin, 2024. Alkis berlin gebaeude. [dataset].

Senatsverwaltung für Stadtentwicklung und Wohnen, 2021. Lebensweltlich orientierte räume. Amt für Statistik Berlin-Brandenburg. URL: https://www.berlin.de/sen/sbw/stadtdaten/stadtwissen/sozialraumorientierte-planungsgrundlagen/lebensweltlich-orientierte-raeume/. [dataset].

Senatsverwaltung für Stadtentwicklung und Wohnen Berlin, 2014. Straßenbefahrung 2014. Geoportal Berlin. URL: https://daten.berlin.de/datensaetze/strassenbefahrung-2014-wms-d4c0abae. [dataset].

Senatsverwaltung für Stadtentwicklung und Wohnen Berlin, 2015. Flächennutzung und stadtstruktur. Geoportal

Berlin. URL: https://daten.berlin.de/datensaetze/stadtstruktur-2015-umweltatlas-wfs-2ff673dc. [dataset].

Smith, I.A., Templer, P.H., Hutyra, L.R., 2023. Water sources for street trees in mesic urban environments. Science of The Total Environment , 168411doi:https://doi.org/10.1016/j.scitotenv.2023.168411.

Tams, L., Paton, E., Kluge, B., 2024. Urban tree drought stress: Sap flow measurements, model validation, and water management simulations. Science of The Total Environment 957, 177221. doi:10.1016/j.scitotenv.2024.177221.

Tams, L., Paton, E.N., Kluge, B., 2023. Impact of shading on evapotranspiration and water stress of urban trees. Ecohydrology 16. doi:10.1002/eco.2556.

Techapinyawat, L., Timms, A., Lee, J., Huang, Y., Zhang, H., 2024. Integrated urban land cover analysis using deep learning and post-classification correction. Computer-Aided Civil and Infrastructure Engineering 39, 3164–3183. doi:https://doi.org/10.1111/mice.13277.

Timm, A., Kluge, B., Wessolek, G., 2018. Hydrological balance of paved surfaces in moist mid-latitude climate – a review. Landscape and Urban Planning 175, 80–91. doi:10.1016/j.landurbplan.2018.03.014.

Tobias, S., Conen, F., Duss, A., Wenzel, L.M., Buser, C., Alewell, C., 2018. Soil sealing and unsealing: State of the art and examples. Land Degrada-

tion & Development 29, 2015–2024. doi:https://doi.org/10.1002/ldr.2919.

Velasquez-Camacho, L., van Doorn, N., Preisler, H., Etxegarai, M., Alas, O., Gonzalez Castro, J.M., de Miguel, S., 2025. Monitoring temporal changes in large urban street trees using remote sensing and deep learning. PLOS One 20, e0326562. doi:10.1371/journal.pone.0326562.

Viswanathan, B., Volder, A., Watson, W.T., Aitkenhead-Peterson, J.A., 2011. Impervious and pervious pavements increase soil co2 concentrations and reduce root production of american sweetgum (liquidambar styraciflua). Urban Forestry & Urban Greening 10, 133–139. doi:10.1016/j.ufug.2011.01.001.

Vrecenak, A., Vodak, M., Fleming, L., 1989. The influence of site factors on the growth of urban trees. Arboriculture & Urban Forestry 15, 206–209. doi:https://doi.org/10.48044/jauf.1989.045.

Watson, G.W., Hewitt, A.M., Custic, M., Lo, M., 2014. The management of tree root systems in urban and suburban settings: A review of soil influence on root growth. Arboriculture & Urban Forestry 40, 193–217. URL: https://auf.isa-arbor.com/content/40/4/193, doi:10.48044/jauf.2014.021, arXiv:https://auf.isa-arbor.com/content/40/4/193.full.pdf.

Wellmann, T., Schug, F., Haase, D., Pflugmacher, D., van der Linden, S.,

2020. Green growth? on the relation between population density, land use and vegetation cover fractions in a city using a 30-years landsat time series. Landscape and Urban Planning 202, 103857. doi:10.1016/j.landurbplan.2020.103857.

Wessolek, G., Kluge, B., 2021. Predicting water supply and evapotranspiration of street trees using hydro-pedo-transfer functions (hptfs). Forests 12, 1010. doi:https://doi.org/10.3390/f12081010.

Whitlow, T., Bassuk, N., 1987. Trees in difficult sites. Arboriculture & Urban Forestry .

Willaredt, M., 2025. High-resolution imperviousness, pavement material and infiltration reduction at street tree catchment scale in Berlin, Germany. ZENODO. doi:10.5281/ZENODO.17316494.

Appendix A. Supplementary Material

Appendix A.1. Dataset descriptions

Appendix A.2. Analysis of completeness of polygon data per catchment

Cropping the polygon-based dataset using tree catchments resulted in some catchments with void areas. Those were identified by comparing the sum of sizes of sub polygons with the total catchment size and classified. Table A.6 provides the values used to classify the completeness of the derived dataset and Figure A.7 in the Appendix shows the distribution of size classes for missing and overlapping polygons.

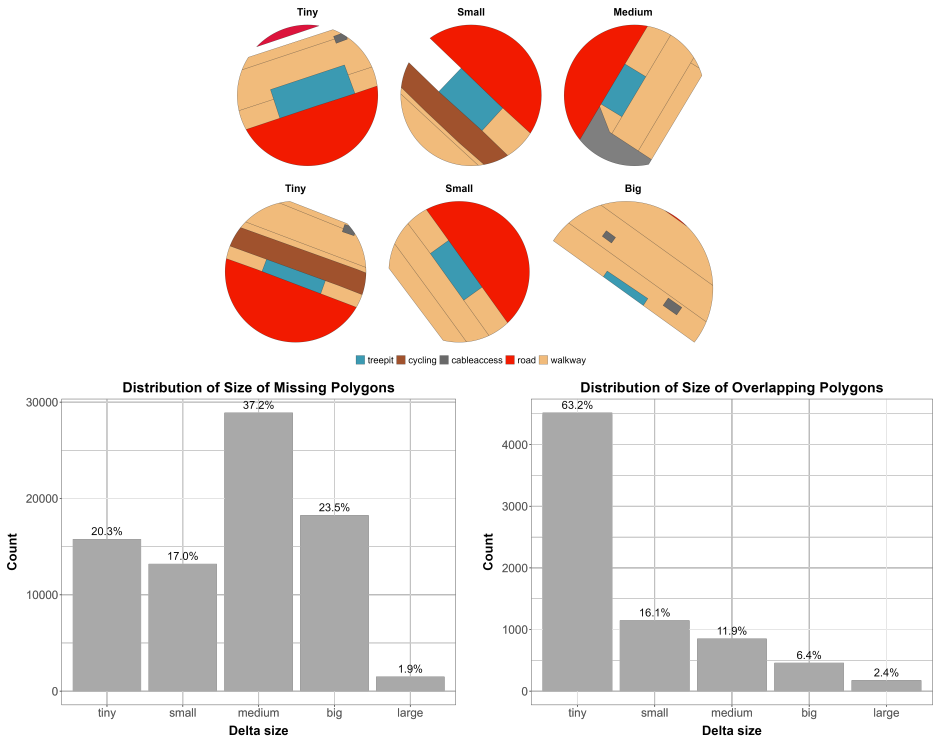

Figure A.7: Upper panel: Examples of tree catchments with missing polygons. Lower panels: Count of size classes of missing and overlapping polygons in dataset. catchments with missing or overlapping polygons classified as tiny (<5 %) were included for the analysis

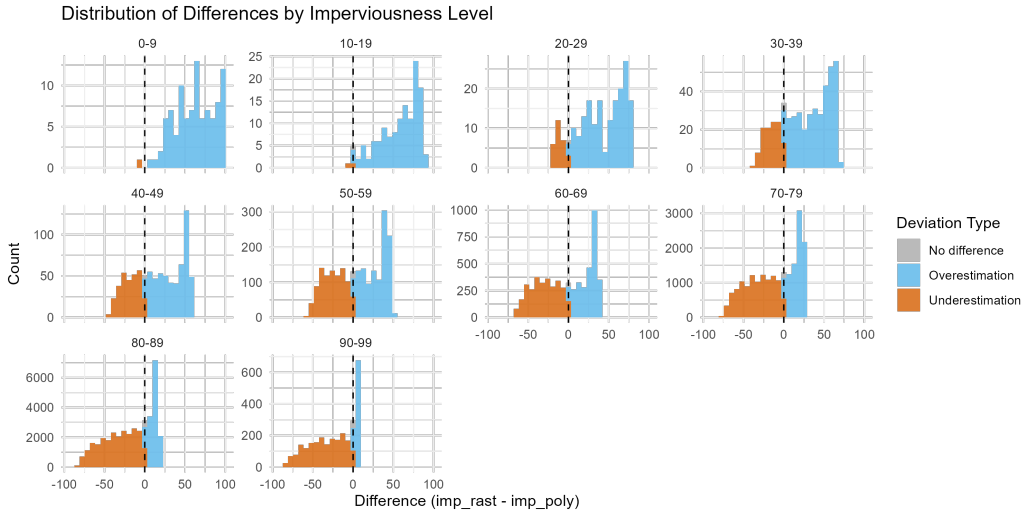

Figure A.8: Disagreement between the two datasets for different ranges of imperviousness

Appendix A.3. Additional figures

Appendix A.4. Analysis of urban form

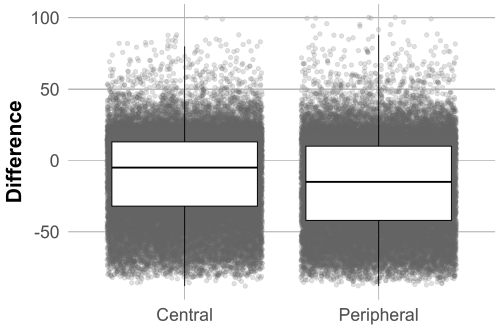

Figure A.9: Boxplot describing difference between data disagreement measured in catchments in centrally located neighborhoods compared to catchments located in peripheral neighborhoods

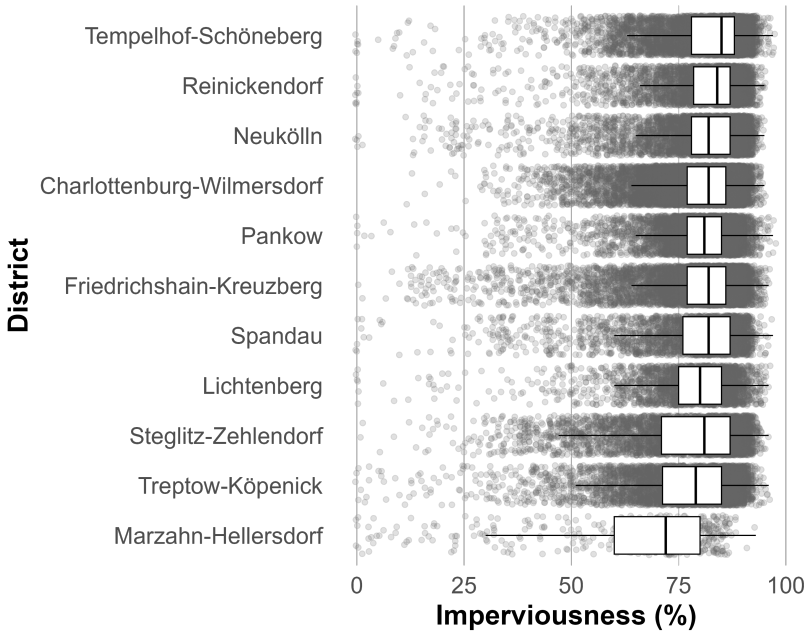

Figure A.10: Boxplot describing difference between data disagreement measured in catchments located in different districts

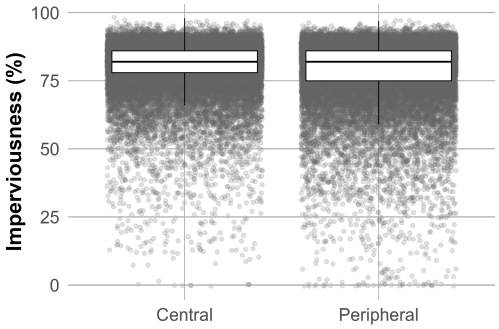

Figure A.11: Boxplot describing imperviousness in catchments in centrally located neighborhoods compared to catchments located in peripheral neighborhoods

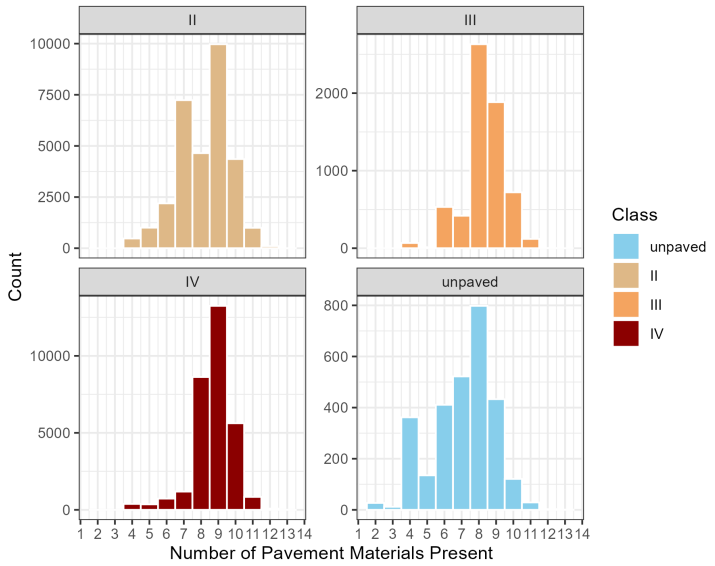

Figure A.12: Histogram illustrates the distribution of the numbers of different pavement materials mapped per catchment.

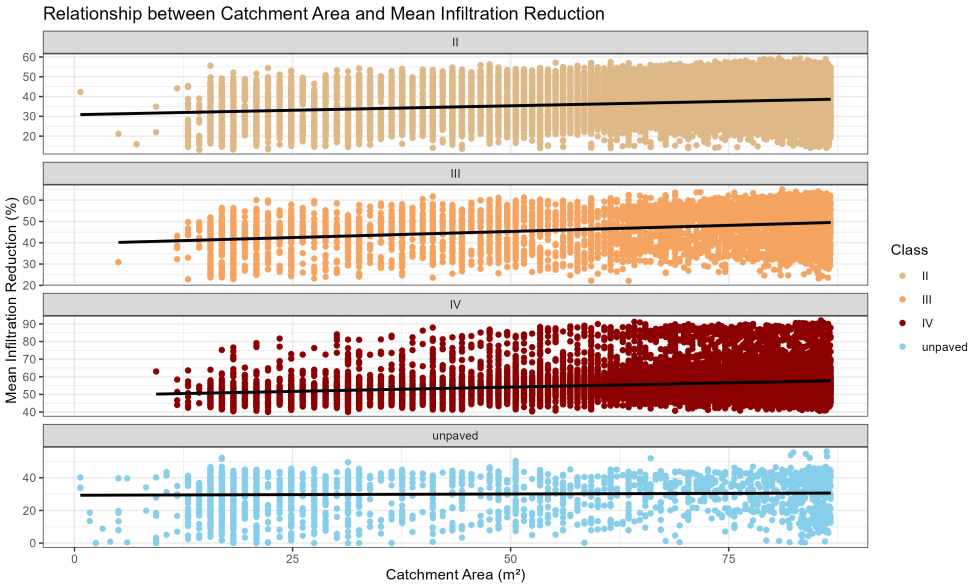

Figure A.13: Relationship between mean infiltration reduction caused by the presence of pavement in a tree catchment and the respective catchment facetted by the dominant material class

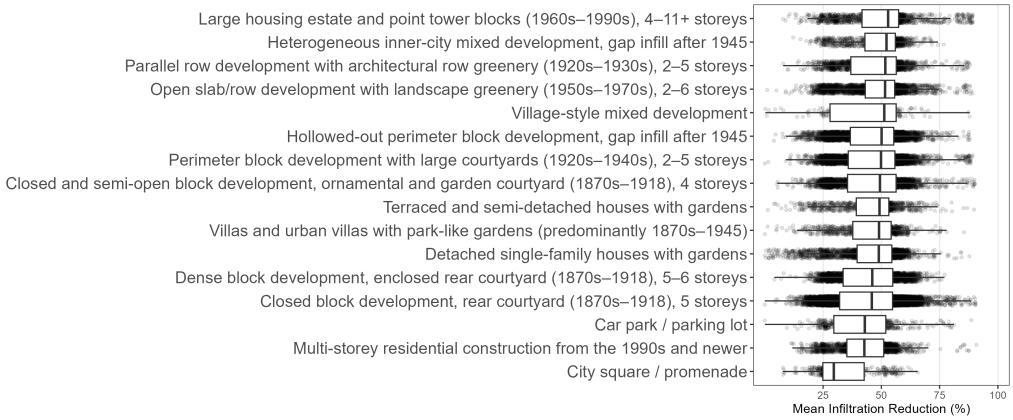

Figure A.14: Distribution of mean infiltration reduction in tree catchments of streets adjacent to blocks characterized by distinct urban form in the City of Berlin.

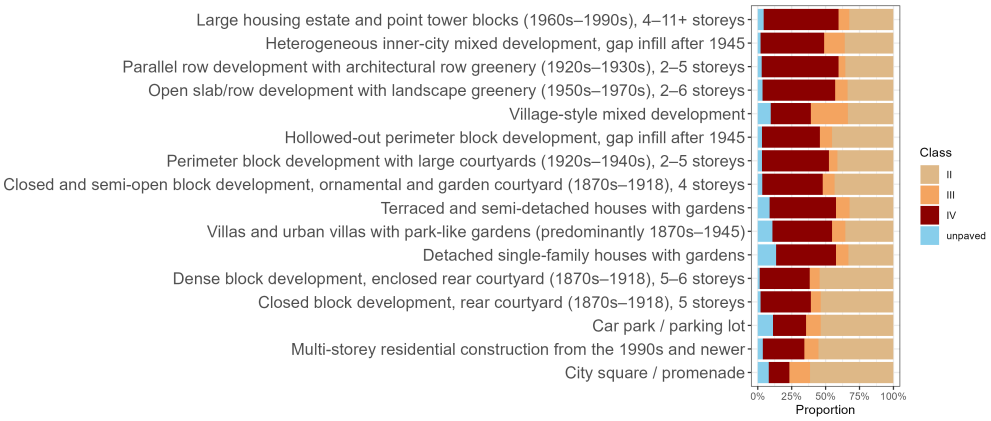

Figure A.15: Proportions of catchments grouped by their dominant material class adjacent to blocks of distinct urban form in the City of Berlin. The order is according to the calculated infiltration reduction

Table A.4: Open spatial datasets used in the study

Dataset title	**Description**
Baumbestand Berlin	Tree inventory, street and park trees, EPSG 25833 ETRS89 / UTM zone 33N, points (Senatsverwaltung für Mobilität, Verkehr, Klimaschutz und Umwelt Berlin, 2024a)
Lebensweltlich orientierte Räume (LOR)	Spatial planning zones in Berlin, EPSG 25833 ETRS89 / UTM zone 33N, polygons (Senatsverwaltung für Stadtentwicklung und Wohnen, 2021)
ALKIS Berlin Gebäude - Buildings layer	Berlin's building footprints, EPSG 25833 ETRS89 / UTM zone 33N, polygons (Senatsverwaltung für Stadtentwicklung, Bauen und Wohnen Berlin, 2024)
Straßenbefahrung 2014[1]	Berlin's public street scape, polygons , EPSG 25833 ETRS89 / UTM zone 33N (Senatsverwaltung für Stadtentwicklung und Wohnen Berlin, 2014)
Grünanlagenbestand Berlin (einschließlich der öffentlichen Spielplätze)	Berlin's parks and recreation green spaces , EPSG 25833 ETRS89 / UTM zone 33N, polygons (Senatsverwaltung für Mobilität, Verkehr, Klimaschutz und Umwelt Berlin, 2024b)
Versiegelung 2021 (Umweltatlas)	Degree of soil sealing on block level, EPSG 25833 ETRS89 / UTM zone 33N (Senatsverwaltung für Stadtentwicklung, Bauen und Wohnen Berlin, 2022)
Stadtstruktur 2015 (Umweltatlas)	Land use types on block level, EPSG 25833 ETRS89 / UTM zone 33N (Senatsverwaltung für Stadtentwicklung und Wohnen Berlin, 2015)
Imperviousness Density 2018	Copernicus high-resolution imperviousness product capturing the percentage of soil sealing, EPSG 3035, raster, res: 10 m (European Environment Agency and European Environment Agency, 2020)

[1] A detailed list of included layers from the dataset in Table A.5

Table A.5: Included layers from dataset Strassenbefahrung 2014, sorted alphabetically surface type mapped in public space together with assigned material properties for those surface types that lack material specification (Senatsverwaltung für Stadtentwicklung und Wohnen Berlin, 2014)

Surface type	**Layer Name**	**Material feature**
bus stop	strassenbefahrung:ca_haltebereich_bus	mapped
bus stop waiting area	strassenbefahrung:cb_haltestellenwartebereich	matched
cable duct	strassenbefahrung:bt_kabelschacht	assigned 00
entrance build	strassenbefahrung:bm_zugangsbauwerk	00
green area	strassenbefahrung:ce_gruenflaeche	assigned 15
parking	strassenbefahrung:ck_parkflaeche	mapped
ped zone	strassenbefahrung:cj_fussgaengerzone	mapped
ramp	strassenbefahrung:cd_rampe	mapped
small building	strassenbefahrung:bu1_kleinbauten_sondernutzung	assigned 00
square	strassenbefahrung:ci_oeffentlicher_platz	mapped
street	strassenbefahrung:cm_fahrbahn	mapped
street bump	strassenbefahrung:bx_fahrbahnschwelle	mapped
traffic divider	strassenbefahrung:cf_trennstreifen	mapped
tree pits	strassenbefahrung:bn_baumscheibe	assigned 14
walkway	strassenbefahrung:cl_gehweg	mapped
walkway cross	strassenbefahrung:by_gehwegueberfahrt	mapped
cycle lane	strassenbefahrung:ch_radweg	mapped

Table A.6: Classification of missing or overlapping areas for analyzing completeness of polygon based imperviousness per catchment

Area in (%)	Class
0	complete
< 5	tiny
< 10	small
< 20	medium
< 50	big
> 50	large